

# A Southern sky search for repeating Fast Radio Bursts using the Australian SKA Pathfinder.

S. Bhandari,<sup>1\*</sup>, K. W. Bannister<sup>1</sup>, C. W. James<sup>2</sup>, R. M. Shannon<sup>3,4</sup>,  
C. M. Flynn<sup>4</sup>, M. Caleb<sup>5</sup>, J. D. Bunton<sup>1</sup>

<sup>1</sup> CSIRO Astronomy and Space Science, PO Box 76, Epping, NSW 1710, Australia

<sup>2</sup> International Centre for Radio Astronomy Research, Curtin University, Bentley, WA 6102, Australia

<sup>3</sup> Centre for Astrophysics and Supercomputing, Swinburne University of Technology, Mail H30, PO Box 218, Hawthorn, VIC 3122, Australia

<sup>4</sup> ARC Centre of Excellence for Gravitational Wave Discovery (OzGrav)

<sup>5</sup> Jodrell Bank Centre for Astrophysics, School of Physics and Astronomy, The University of Manchester, Manchester M13 9PL, UK

Accepted XXX. Received YYY; in original form ZZZ

## ABSTRACT

We have conducted a search for bright repeating Fast Radio Bursts in our nearby Universe with the Australian Square Kilometer Array Pathfinder (ASKAP) in single-dish mode. We used eight ASKAP 12-m dishes, each equipped with a Chequerboard Phased Array Feed forming 36 beams on the sky, to survey  $\sim 30,000$  deg<sup>2</sup> of the southern sky ( $-90^\circ < \delta < +30^\circ$ ) in 158 antenna days. The fluence limit of the survey is 22 Jy ms. We report the detection of FRB 180515 in our survey. We found no repeating FRBs in a total mean observation of 3 hrs per pointing divided into one hour intervals, which were separated in time ranging between a day to a month. Using our non-detection, we exclude the presence of a repeating FRB similar to FRB 121102 closer than  $z = 0.004$  in the survey area — a volume of at least  $9.4 \times 10^4$  Mpc<sup>3</sup> — at 95% confidence.

**Key words:** surveys – intergalactic medium – pulsars: general

## 1 INTRODUCTION

The capability of instantaneously observing a large area of the sky has not only ramped up the detection of millisecond fast radio bursts (FRBs) but also diversified the current FRB population (Petroff et al. 2016). FRBs have the capacity to be used as cosmological probes and offer an entirely new means of addressing questions such as the magnetic field of the intergalactic medium, the well-known problem of the “missing baryons” (McQuinn 2014; Ioka 2003) and the dark energy density (Zhou et al. 2014) by providing distances, when localised to distant galaxies and/or other sources, pending the nature of FRB hosts. The Australian Square Kilometer Array Pathfinder (ASKAP), a radio array consisting of 36×12 m dishes and currently being commissioned in the Murchison Widefield Observatory have proved to be an excellent instrument for wide-field and blind searches for FRBs. It is equipped with Chequerboard Phased Array Feeds (Hay & O’Sullivan 2008, PAF) making it a fast 21-cm survey machine.

The Commensal Real-Time ASKAP Fast-Transients (Macquart et al. 2010, CRAFT) latitude-50 survey has de-

tected 20 new FRBs, surveying a large field of view in fly’s eye mode (150 – 270 deg<sup>2</sup>) (Shannon et al. 2018). The more luminous and relatively low dispersion measure sample of these ASKAP FRBs complements the distant events found in narrow-field and more sensitive surveys, e.g. Bhandari et al. (2018); Keane et al. (2018). These investigations of the brighter and closer FRB population are crucial in understanding the energetics of their radio emission. Additionally, detections with ASKAP permit robust measurements of the burst fluences because of the tight-packed beam configuration, whereas fluences obtained at other telescopes, such as Parkes, are generally lower limits.

Another advantage of ASKAP’s high survey speed is the ability to re-observe the surveyed area, especially when it comes to fast transient searches including single pulse searches for pulsars. This can potentially lead to discoveries of new intermittent, nulling or sporadic sources. An extensive follow-up campaign of the FRB 121102, first detected in the PALFA survey by Arecibo in 2014 (Spitler et al. 2014), resulted in the discovery of the repeating pulses, making it the first repeating FRB (Spitler et al. 2016). Furthermore, its repeating nature led to an unambiguous localisation to a low-metallicity, dwarf host galaxy at  $z = 0.19$  (Chatterjee et al. 2017; Tendulkar et al. 2017). Recently, six

\* E-mail: shivani.bhandari@csiro.au

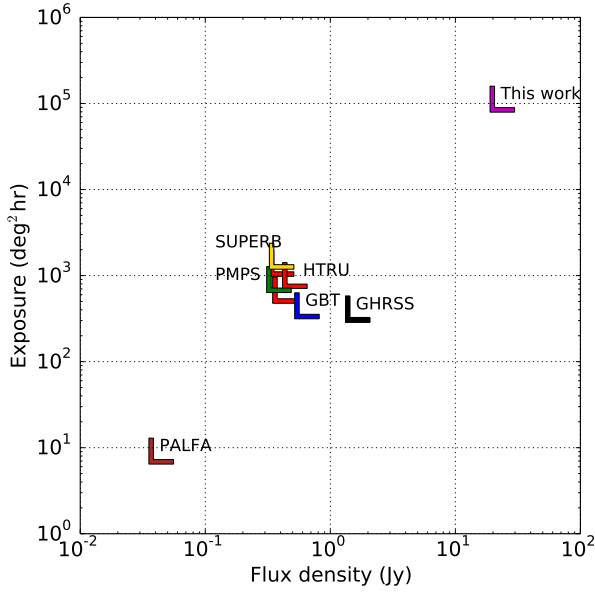


**Figure 1.** The phase space of sensitivity versus survey speed probed by current and archival transient surveys. The upper limits for various transient surveys are presented in this plot. The high, medium and low latitude High Time Resolution Universe Survey (HTRU) at Parkes are marked as red points (Keith et al. 2010). Other surveys at the Parkes radio telescope including SUPERB (Keane et al. 2018) and PMPS (Manchester et al. 2001) are shown as yellow and green points. Brown, blue and black data points presents the surveys conducted at the Arecibo (Deneva et al. 2009; Patel et al. 2018, PALFA), the Green Bank telescope (Stovall et al. 2014, GNBCC) and the Giant Metrewave Radio telescope (Bhattacharyya et al. 2016, GHRSS). The CRAFT all-sky survey using the ASKAP (this work) is presented using magenta data point, which explores a wide and shallow part of the phase space.

repeating pulses were detected from FRB 180814.J0422+73 (Amiri et al. 2019b), one of the 13 FRBs reported by CHIME down to 400 MHz (Amiri et al. 2019a). The detection of the FRB 180814.J0422+73 hints at the existence of two classes of FRBs (repeating and non-repeating). Even though the spectral and temporal properties of the pulses observed from FRB 121102 and FRB 180814.J0422+73 are consistent with those observed for putative non-repeating FRBs (Farah et al. 2018; Ravi et al. 2016), the extremely high rotation measure observed for FRB 121102 (Michilli et al. 2018) differentiates the two speculated classes of FRBs.

The CRAFT collaboration has conducted an all-southern-sky survey with ASKAP leveraging its high survey speed and wide-field of view. In this paper we present the results our survey. In Section 2 we describe the observations, survey parameters and data reduction methods. We present our results including the discovery of FRB 180515 in Section 3. Section 4 uses the non-detection of a repeating FRB to limit the number of objects similar to FRB 121102 in the local Universe. We describe our conclusions in Section 5.

## 2 SURVEY OVERVIEW.

The main goal of the CRAFT all-sky survey was to search for nearby bright repeating FRBs by re-observing the sky mul-

tiply times with different cadences. Figure 1 presents the phase space probed by high time resolution surveys conducted by different telescopes. The CRAFT all-sky survey with ASKAP explores a different region of this phase space, targeting the most energetic and/or closest FRBs over the broadest region of sky.

### 2.1 Observations and Survey parameters

The observations were conducted in ASKAP’s fly’s eye mode, with each antenna pointing to a different position on the sky. The voltages measured by the PAFs are amplified, digitized and filtered into 336 coarse channels of 1 MHz width. The beam-former for each antenna constructs 36 beams by summing and weighting signals from individual PAF elements. Each beam has a FWHM of  $\sim 1$  deg and 36 beams are overlapped to yield a field of view  $\sim 30$  deg<sup>2</sup> at 1.4 GHz (Hotan et al. 2014). We have used eight ASKAP dishes, simultaneously observing  $\sim 240$  deg<sup>2</sup> of the sky. The beams were arranged in a the “closepack36” configuration with a pitch of  $0.9^\circ$  and  $60^\circ$  rotation on the sky. The survey covers the full sky visible to ASKAP in 1286 pointings, which we divided into three regions with declinations:  $-80^\circ$  to  $-30^\circ$  (AS1),  $-30^\circ$  to  $0^\circ$  (AS2) and  $0^\circ$  to  $30^\circ$  (AS3), also shown in Figure 2. The polarization axis (the roll axis of the dish) was set to  $120^\circ$  and  $-60^\circ$  for pointings north and south of declination  $-30^\circ$  respectively, resulting in a beam pattern on the sky with minimum overlap, as shown Figure 3.

The observations were conducted between 2018 March 08 and 2018 May 21 with a total on-sky time of  $\sim 158$  antenna days. Each pointing was observed for a minimum duration of one hour. The mean total observation time per pointing for the survey was  $\sim 3$  hrs as presented in the top panel of the Figure 4. The pointings were re-observed at least once; the revisit time varied from a day to a month, with a mean time of  $\sim 18$  days as seen in the bottom panel of Figure 4. The technical specifications of the survey are listed in Table 1.

The observation strategy was motivated by the clustered nature of the repeating pulses from FRB 121102 (Scholz et al. 2016; Law et al. 2017; Gajjar et al. 2018). Oppermann et al. (2018) adopted a Weibull distribution to explain the observed clustering of pulses and also proved that observations interspersed with gaps have a higher chance of detecting a burst than a continuous observations with the same total time.

Scaling from the results of Shannon et al. (2018), who reported detection of 20 FRBs in  $\sim 1300$  antenna days, we expected to find  $\sim 2.4$  FRBs in our survey of 158 antenna days. One such FRB was found (FRB 180515), consistent with this estimate (see Section 3.1).

### 2.2 Data reduction pipeline

The square-law-detected voltages from the beamformers are integrated to yield a time resolution of 1.265 ms. The filterbank data is then searched offline for bright single pulses using FREDDA (K. W. Bannister 2019, in preparation), the GPU-based implementation of the Fast Dispersion Measure Transform algorithm (Zackay & Ofek 2017, FDMT). Each block of data is flagged and rescaled before performing the FDMT operation independently on each beam. The search

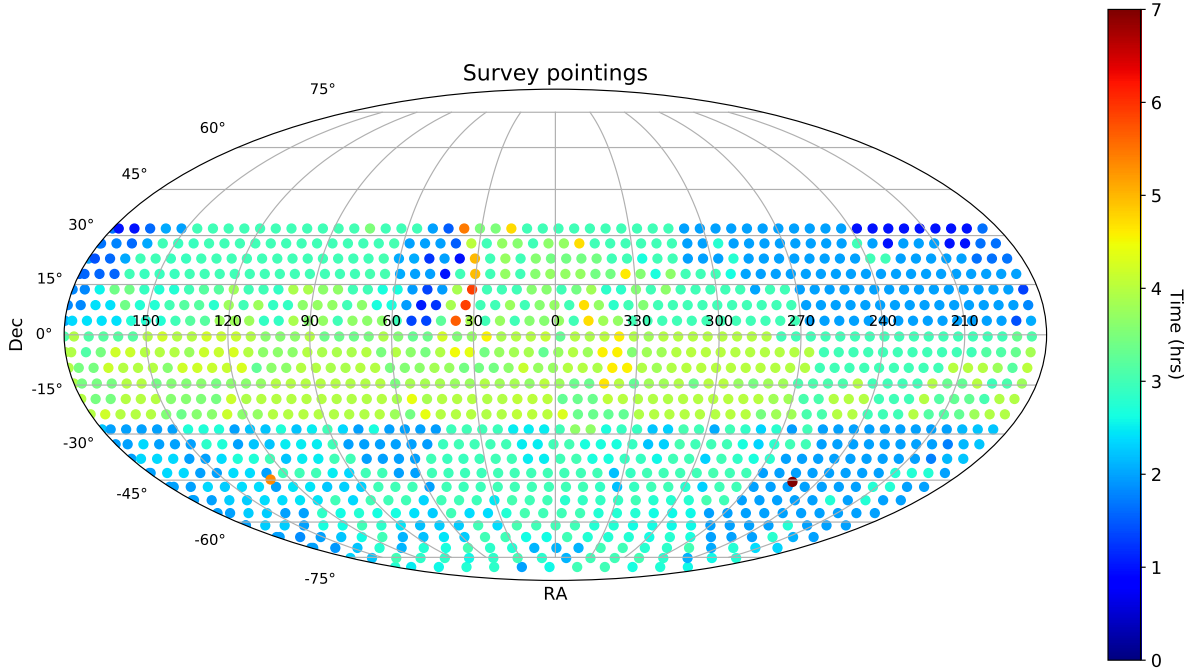


**Figure 2.** An airtoll projection of 1286 survey pointings covering  $\sim 30000 \text{ deg}^2$  of the southern sky. A pointing consists of a set of 36 beams arranged in a closepack pattern, observing a given position on the sky. They are colour coded by their total observation time in hours. The typical total time spent on a given position is  $\sim 3$  hours (see Figure 4)

**Table 1.** The specifications of the CRAFT All-Sky survey

|                                        |                                  |
|----------------------------------------|----------------------------------|
| Region AS1                             | $-80^\circ < \delta < -30^\circ$ |
| Region AS2                             | $-30^\circ < \delta < 0^\circ$   |
| Region AS3                             | $0^\circ < \delta < 30^\circ$    |
| $\tau_{\text{obs}}$ per pointing (sec) | 3600                             |
| SEFD (Jy)                              | $\sim 2000$                      |
| Total pointings                        | 1286                             |
| $N_{\text{beams}}$ per pointing        | 36                               |
| Bandwidth (MHz)                        | 336                              |
| $\tau_{\text{samp}}$ (ms)              | 1.265                            |
| $\Delta\nu_{\text{chan}}$ (MHz)        | 1                                |
| Centre Frequency (GHz)                 | 1.32                             |
| $N_{\text{chans}}$                     | 336                              |

for single pulses is performed in 4096 dispersion measure trials with DM ranging from  $0-3763 \text{ pc cm}^{-3}$  and boxcar width trials in the range of 1 – 32 samples. The known pulsar candidates are disregarded after comparing them with pulsar catalogue (Qiu et al, submitted to MNRAS) and candidates with  $S/N > 12$  and width  $< 12$  samples are classified as FRB candidates, which are manually inspected. A detailed description of the search pipeline is in [Bannister et al. \(2017\)](#).

### 3 RESULTS

We found one FRB in our survey, which is consistent with the expectation within the errors. No repeats of this FRB were found.

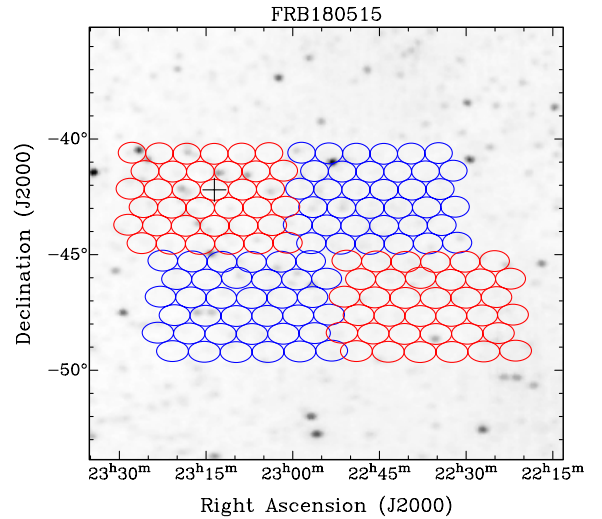


**Figure 3.** A plot of the closepack36 footprint arrangement of 36 beams on the sky for four pointings. Greyscale image is the CHIPASS 1.4 GHz radio continuum map, different colours represent different pointings, and the black cross represents the position of FRB 180515. The symbols represent the FWHM of the beam.

#### 3.1 Detection of FRB 180515

FRB 180515 was discovered on 2018 May 15 UT 21:57:26.485 in the CRAFT AS1 region survey by antenna 15 after observing for 45 antenna days in the fly’s eye mode. It was

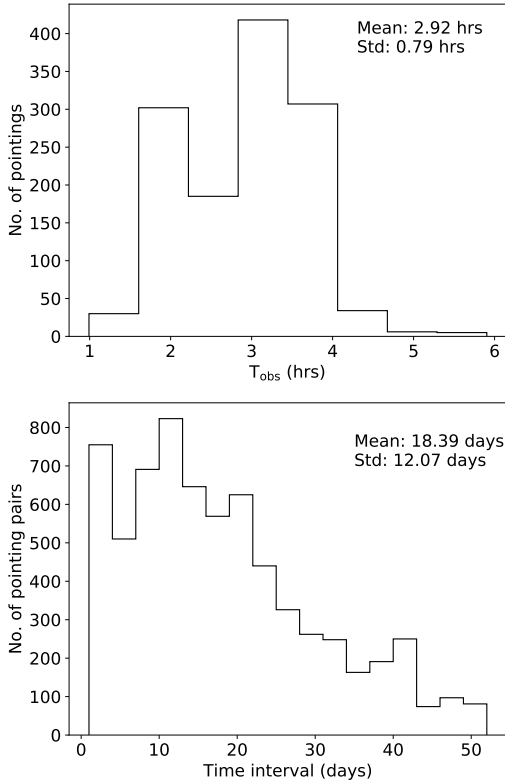


**Figure 4.** Top panel: Histogram of observation times for survey pointings. The mean observation time is 2.92 hrs. Bottom panel: Histogram of the time intervals between re-observation of a given pointing. This varies from a day to a month with a mean revisit time of 18 days.

detected in beam 20 with a S/N of 12.1 at RA: 23:13:12 and DEC:  $-42:14:46$ ,  $4.9'$  away from the beam centre, with the localisation error region of  $7'$  at the 90% confidence level. (Figure 5). The burst has a dispersion measure (DM) of  $355.2 \text{ pc cm}^{-3}$  and is  $1.9(4)$  ms wide. It has a fluence of  $46(2)$  Jy ms where the uncertainty in the position is accounted for in determining the uncertainty in the fluence. This is discussed in detail in Bannister et al. (2017). The burst is only marginally brighter in the lower half of the band Figure 6. We have accounted for the offset position from the beam centre and the known gain variations in the band. This is discussed in the supplementary information of Shannon et al. (2018). The burst does not show significant scattering and upper limit is presented in Table 2.

### 3.2 Maximum redshift and isotropic energy of FRB 180515.

The total DM of an FRB ( $DM_{\text{total}}$ ) can be expressed as:

$$DM_{\text{total}} = DM_{\text{MW(disk)}} + DM_{\text{MW(halo)}} + DM_{\text{IGM}} + DM_{\text{Host}} \quad (1)$$

where  $DM_{\text{MW(disk)}}$  is the DM contribution from the Milky Way disk,  $DM_{\text{MW(halo)}}$  is the Milky Way halo contribution,  $DM_{\text{IGM}}$  is contribution from the intergalactic medium and  $DM_{\text{Host}}$  is the FRB host galaxy contribution. Using the Galactic models of NE2001 (Cordes & Lazio 2002) and YWM16 (Yao et al. 2017), we obtain a Milky Way disk DM contribution of  $\sim 33 \text{ pc cm}^{-3}$  and  $\sim 19 \text{ pc cm}^{-3}$  respectively

**Table 2.** The measured and model dependent properties of FRB 180515.

| Measured Properties                            |                               |
|------------------------------------------------|-------------------------------|
| Event time at 1.4 GHz UTC                      | 2018-15-05 21:57:26.485       |
| ASKAP beam                                     | 20                            |
| Beam centre (Ra, Dec) (J2000)                  | 23:13:33.8, $-42:11:51.3$     |
| FRB (Ra, Dec) (J2000)                          | 23:13:12, $-42:14:46$         |
| Localisation error                             | $7'$ radius                   |
| Galactic coordinates ( $\ell$ , $b$ )          | $349.5^\circ$ , $-64.9^\circ$ |
| Signal to noise ratio, (S/N)                   | 12.1                          |
| Dispersion measure, DM ( $\text{pc cm}^{-3}$ ) | $355.2(5)$                    |
| Fitted width (ms)                              | $1.9(4)$                      |
| Scattering time (ms)                           | $< 0.38^{+0.10}_{-0.12}$      |
| Measured fluence (Jy ms)                       | $46(2)$                       |
| Model-dependent properties                     |                               |
| $DM_{\text{NE2001}}$ ( $\text{pc cm}^{-3}$ )   | $\sim 33$                     |
| $DM_{\text{YWM16}}$ ( $\text{pc cm}^{-3}$ )    | $\sim 19$                     |
| Max. inferred $z$                              | 0.2                           |
| Max. comoving distance (Gpc)                   | 0.9                           |
| Max. luminosity distance (Gpc)                 | 1.1                           |
| Max. isotropic energy ( $10^{33}$ J)           | 1.6                           |

along the line of sight for FRB 180515. We assumed Milky Way halo and host galaxy DM contribution to be  $\sim 12 \text{ pc cm}^{-3}$  and  $\sim 45 \text{ pc cm}^{-3}$  (Mahony et al. 2018; Xu & Han 2015). This results in an intergalactic medium contribution in the range  $265 < DM_{\text{IGM}} < 280 \text{ pc cm}^{-3}$ . For a given excess DM, assuming the likelihood of  $DM_{\text{IGM}}$  along a sightline to be a Gaussian with redshift-evolving mean and variance and a homogeneous prior redshift distribution for FRBs, the most probable redshift can be calculated using the methods described in Walker et al. (2018). For  $265 < DM_{\text{IGM}} < 280 \text{ pc cm}^{-3}$ , this redshift range is  $0.255 < z_{\text{max}} < 0.269$ . A search in the WISExSCOS Photometric Redshift Catalogue (Bilicki et al. 2016, WISExSCOSPZ) in the localization region with redshift constrained to  $z < 0.27$  resulted in 35 galaxies brighter than the survey magnitude limit  $I = 18.5$ . The galaxies have redshifts in the range of  $0.04 - 0.259$  and they reside in the region of non-AGN ‘‘spirals’’ in the WISE colour-colour plot (Wright et al. 2010) as shown in the Figure 7. However, we lack confidence in associating any galaxy to FRB 180515.

The in-band isotropic energy of an FRB using  $\Lambda$ CDM cosmology (Planck Collaboration et al. 2016) can be expressed as:

$$E(J) = \frac{\mathcal{F}_{\text{obs}} \times \text{BW} \times 4\pi D_L^2 \times 10^{-29}}{(1+z)^{2-\alpha}} \quad (2)$$

where  $\mathcal{F}_{\text{obs}}$  is the observed fluence for an FRB in Jy ms, BW is the bandwidth at ASKAP in Hz,  $D_L$  is the luminosity distance in metres,  $z$  is the redshift, and  $\alpha$  is the spectral index of the source ( $F \propto \nu^\alpha$ ). We assume a flat spectrum for FRBs i.e.,  $\alpha = 0$ .

Using equation 2 for FRB 180515, we obtain an isotropic energy of  $1.6 \times 10^{33}$  J. These properties are also listed in Table 2.

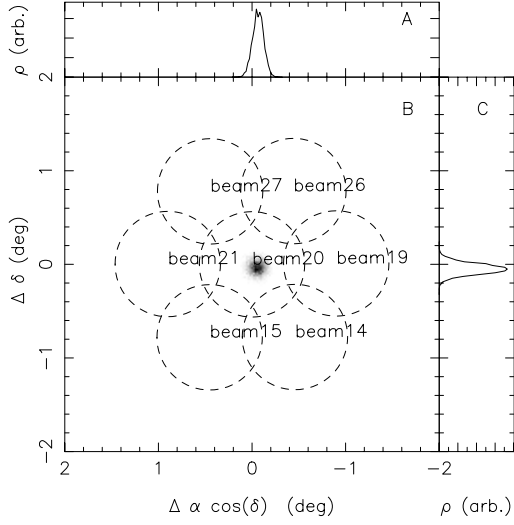


**Figure 5.** Constraints on position of FRB 180515. Panels A, B and C show the one and two-dimensional posterior distributions for burst position. The centre (0,0) in panel B is the best position of the FRB which is RA: 23:13:12 and DEC:  $-42:14:46$ ,  $4.9'$  away from the beam centre. The marginal adjacent beam detections ( $S/N < 3$ ) are stronger in beams 14, 15 and 19 than they are in beams 21, 26 and 27, hence the centroid of the posterior distribution has been shifted slightly in the direction of the former set of beams. This FRB has an positional uncertainty of a radius of  $7'$  at the 90% confidence level.

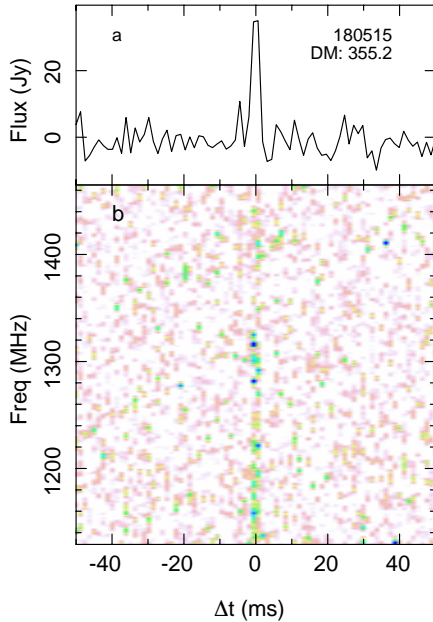


**Figure 6.** Panel A: The pulse profile of FRB 180515 de-dispersed to a DM of  $355.2 \text{ pc cm}^{-3}$ . We note a  $3\sigma$  precursor spike, which is consistent with noise. Panel B: The FRB's dynamic spectrum. The colour map is set to range from the mean to  $4\sigma$  of the off-pulse intensity. The FRB is similar to other FRBs found at ASKAP at high Galactic latitude.

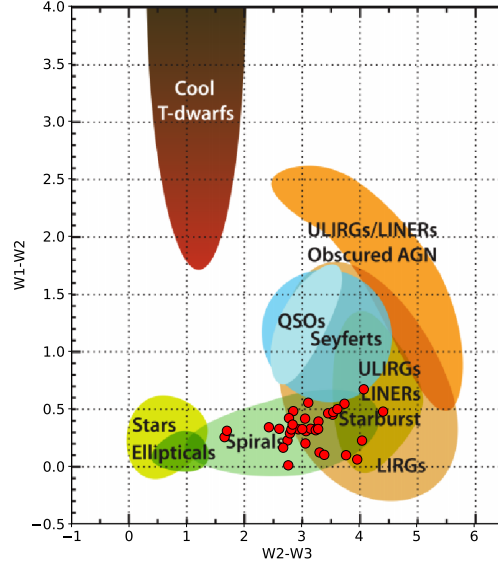


**Figure 7.** A plot of the WISE colours of 35 galaxies (red points) detected in WISExSCOSPZ catalogue in the FRB 180515 position error region, overlaid on the plot taken from Wright et al. (2010). The galaxies reside in the spiral region of the plot.

#### 4 LIMITS ON REPEATING FRBS IN THE LOCAL UNIVERSE

No repeat FRBs were found in the survey. The observed rate of FRBs from a population of progenitors producing repeat bursts can be described in terms of intrinsic progenitor properties — in particular, the repetition rate  $R$  as a function of burst energy — and the population distribution, which we characterise as the redshift-dependent number density per co-moving cubic Mpc,  $\rho(z)$ . Given the exceptionally broad range of parameter space that could describe a repeating FRB (rate, time distribution, pulse strength, frequency structure, etc.), we use the first known repeater, FRB 121102, to characterise all potentially repeating FRBs, and use our observations to limit the density of similar objects in the local Universe. Knowledge of the second known repeater, FRB 180814.J0422+73 (Amiri et al. 2019a,b), remains too rudimentary to use this object as a benchmark. The statistical analysis of this object is described in James (2019) which primarily uses the results of Law et al. (2017) and Gajjar et al. (2018) to model the cumulative brightness distribution of bursts via:

$$\begin{aligned}
 R(E > E_0) &= R_0 \left( \frac{E}{E_0} \right)^\gamma & (3) \\
 R_0 &= 7.4 \text{ day}^{-1} \\
 E_0 &= 1.7 \cdot 10^{38} \text{ erg} \\
 \gamma &= -0.9 & (4)
 \end{aligned}$$

for burst energy  $E$ , time-averaged rate  $R$ , and index of the power law slope of burst energies,  $\gamma$ . This is broadly consistent with the model of intrinsic properties presented by Law et al. (2017).

To examine the dependence of resulting limits on FRB properties, the limits are recalculated with  $R_0$  reduced tenfold, i.e.  $R_0 = 0.74 \text{ day}^{-1}$ .

The arrival time distribution of bursts from FRB 121102 is clearly non-Poissonian in time and has been modeled as a Weibull distribution by [Oppermann et al. \(2018\)](#) based on 80 hr of observations during which only 17 pulses were detected. However, more recently [Zhang et al. \(2018\)](#) show that the arrival time statistics may be indeed be more Poissonian than previously thought to be, especially during the ‘active’ state of the source. We note that observational biases may play a role in skewing our perception of its activity.<sup>1</sup> Even with a Weibull distribution that shows correlated arrival times with Arecibo, multiple regular short observations reduce a clustered repeating source to a near-Poisson process.

Here, we consider only the case of Poissonian arrival statistics, and refer readers to [Connor et al. \(2016\)](#) for a more extensive discussion of how non-Poissonian statistics will interact with the time-distribution of our observations reported in Figure 4. Naively characterising FRB 121102 as being active or inactive (e.g. the ‘early 2016’ vs ‘late 2016’ periods of [Law et al. \(2017\)](#), or the final hour versus the first five hours of [Spitler et al. \(2018\)](#)), with some probability  $p_{\text{active}}$  over the timescales reported in Figure 4, will weaken our resulting limits by a factor of  $1/p_{\text{active}}$ .

#### 4.1 Deriving limits

We place limits on the population of repeating FRBs using our non-observation of repeated pulses, using the method of [James \(2019\)](#). The number of observed single FRBs — here, one — can also be used to limit the number of repeating sources, e.g. in the case of many objects repeating at low rates. Using single pulses will always result in a more powerful method, simply because it uses more information.

The former method is more robust however, in that it is not affected by the presence of a population of cataclysmic sources in addition to repeating sources, at least until the observed burst rate is so high that there is a non-zero probability of a chance coincidence of FRBs from the same location with the same DM.

Following [James \(2019\)](#), if a time  $T_{\text{obs}}$  is spent on-source, then the required intrinsic rate  $R_{\text{lim}}$  to exclude the presence of a repeater is given by:

$$R_{\text{lim}} = (1+z) \frac{\lambda_{\text{lim}}}{T_{\text{obs}}} \quad (5)$$

where the factor of  $(1+z)$  is due to the time-dilation effects of redshift and  $\lambda_{\text{lim}} = 4.84$  is a Poissonian expectation value for an observation of 2 or more bursts from a repeating object at 95% confidence.

The value of  $E_{\text{lim}}$ , above which the repetition rate is  $R_{\text{lim}}$ , can be found by inverting equation 3:

$$\begin{aligned} E_{\text{lim}} &= E_0 \left( \frac{R_{\text{lim}}}{R_0} \right)^{\frac{1}{\gamma}} \\ &= E_0 (1+z)^{\frac{1}{\gamma}} \left( \frac{\lambda_{\text{lim}}}{T_{\text{obs}} R_0} \right)^{\frac{1}{\gamma}}. \end{aligned} \quad (6)$$

However, intrinsic pulses of strength  $E_{\text{lim}}$  must be observable, being a function of  $F$  and  $z$ . Given a threshold  $F_{\text{th}}$ , there

will exist a unique  $z_{\text{lim}}$  satisfying the condition that pulses of intrinsic strength  $E_{\text{lim}}$  are just observable at threshold  $F_{\text{th}}$  when generated at a redshift of  $z = z_{\text{lim}}$ .

Using equation 2 to substitute  $E_{\text{lim}}$  for an expression involving  $z$  and  $F_{\text{th}}$ , we find:

$$(1+z_{\text{lim}})^{\alpha-2-\frac{1}{\gamma}} D_L^2(z_{\text{lim}}) = \frac{E_0}{4\pi F_{\text{th}} \text{BW}_{\text{obs}}} \left( \frac{\lambda_{\text{lim}}}{T_{\text{obs}} R_0} \right)^{\frac{1}{\gamma}}. \quad (7)$$

where  $\text{BW}_{\text{obs}}$  is the observation bandwidth (here, 336 MHz).

Using the closepack36 beam sensitivities from [James et al. \(2018\)](#) to calculate  $F_{\text{th}}$  as a function of solid angle  $\Omega$ , equation 7 can be used to reduce the variables of  $T_{\text{obs}}$  and direction-dependent beam sensitivity to a single function,  $\Omega(z_{\text{lim}})$ , describing the solid angle  $\Omega$  in which the survey would have detected a repeating FRB at a given level of confidence for all  $z \leq z_{\text{lim}}$ . The total solid angle  $\Omega_{\text{lim}}(z)$  and volume  $V_{\text{lim}}$ , over which the presence of a repeating FRB can be excluded are given by [James \(2019\)](#):

$$\Omega_{\text{lim}}(z) = \int_{z_{\text{lim}}=z}^{\infty} \Omega(z_{\text{lim}}) dz_{\text{lim}} \quad (8)$$

and

$$V_{\text{lim}} = \int_0^{\infty} \Omega_{\text{lim}}(z) D_H \frac{(1+z)^2 D_A^2}{E(z)} dz. \quad (9)$$

The integrand in equation 9 represents the comoving volume element, where  $D_A$  is the angular diameter distance,  $D_H$  the Hubble distance, and  $E(z)$  represents the Hubble parameter as a function of redshift. The results are shown in Figure 8. The left panel shows the solid angle of sky in steradians as a function of the limiting redshift  $z_{\text{lim}}$ , and allows us to exclude the presence of a repeating FRB with similar properties to FRB 121102 and south of declination  $\delta = +30^\circ$  within  $z < 0.004$  at 95% confidence. The right panel shows the results of integrating equation 9, to yield the 95% confidence limit on the surveyed volume as a function of redshift. We exclude the presence of a repeating FRB with properties similar to FRB 121102 in a volume,  $V_{\text{lim}}$  of not less than  $9.4 \times 10^4 \text{ Mpc}^3$ .

For FRBs repeating at different rates, the limited volume varies approximately as  $(R_0^{-\frac{1.5}{\gamma}})$  (in Euclidean space). For  $R_0 = 0.74 \text{ day}^{-1}$ , it is  $1.6 \times 10^3 \text{ Mpc}^3$ .

## 5 CONCLUSIONS

We have conducted an all-sky survey with ASKAP to search for bright repeating FRBs in our local Universe. We observed each field for at least one hour and re-observed a given field mostly three times with cadence ranging from a day to a month. We found an FRB 180515 in our AS1 survey which has similar spectral features as other sample of ASKAP FRBs. However, we did not find any repeating FRBs. We used this non-detection to exclude the presence of FRB 121102 like sources within  $z = 0.004$  at 95% confidence over the entire survey region, and calculated a limiting volume of  $9.4 \times 10^4 \text{ Mpc}^3$ , assuming the arrival times of FRB 121102 follow Poisson statistics. The limits are relatively weaker for more general distributions, such as Weibull.

<sup>1</sup> For instance, the only article reporting a non-detection at radio wavelengths appears as a Research Note ([Price et al. 2018](#)).

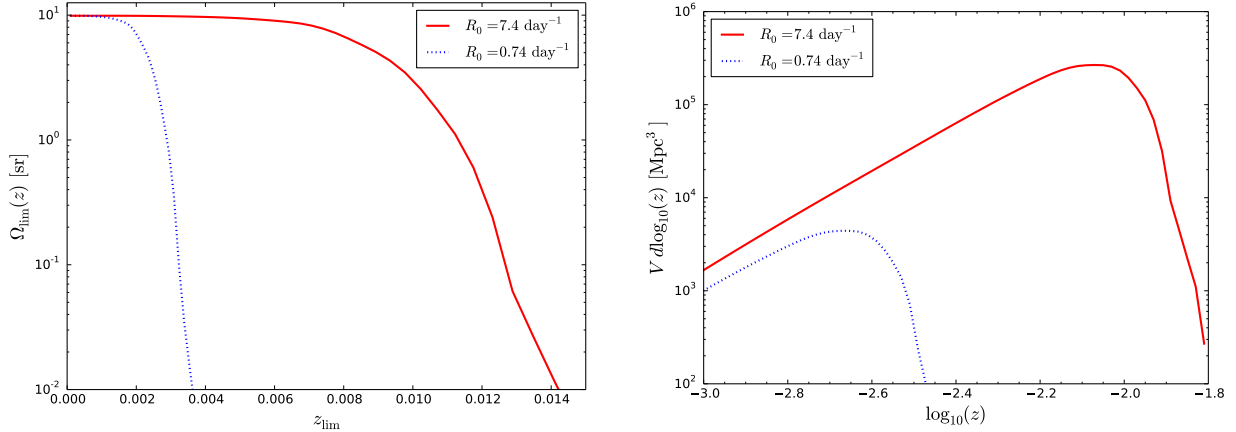


**Figure 8.** Left panel: Solid angle  $\Omega_{\text{lim}}(z)$  over which the presence of a repeating FRB similar to FRB 121102 ( $R_0 = 7.4 \text{ day}^{-1}$ ), and one with reduced rate  $R_0 = 0.74 \text{ day}^{-1}$ , within redshift  $z_{\text{lim}}$  can be excluded at 95% confidence level (C.L.). Right panel: The differential volume in which the presence of a repeating FRB can be excluded at 95% confidence level (C.L.) as a function of redshift,  $z$ .

## ACKNOWLEDGEMENTS

The Australian SKA Pathfinder is part of the Australia Telescope National Facility which is managed by CSIRO. Operation of ASKAP is funded by the Australian Government with support from the National Collaborative Research Infrastructure Strategy. ASKAP uses the resources of the Pawsey Supercomputing Centre. Establishment of ASKAP, the Murchison Radio-astronomy Observatory and the Pawsey Supercomputing Centre are initiatives of the Australian Government, with support from the Government of Western Australia and the Science and Industry Endowment Fund. We acknowledge the Wajarri Yamatji people as the traditional owners of the Observatory site. SB would like to thank the anonymous referee for their comments and suggestions. SB would also like to thank Wael Farah for the scattering fit of the reported FRB and Charlie Walker for estimating the most probable redshift for a given DM contribution from the IGM. KB and RMS acknowledge the support of the Australian Research Council through grant DP18010085. RMS acknowledges salary support from the ARC through grants FL150100148 and CE17010004. CWJ acknowledges the support of the Australian Research Council Centres of Excellence for All Sky Astrophysics (CAASTRO, CE110001020)

## REFERENCES

- Amiri M., et al., 2019a, *Nature*, 566, 230  
Amiri M., et al., 2019b, *Nature*, 566, 235  
Bannister K. W., et al., 2017, *ApJ*, 841, L12  
Bhandari S., et al., 2018, *MNRAS*, 475, 1427  
Bhattacharyya B., et al., 2016, *ApJ*, 817, 130  
Bilicki M., et al., 2016, *ApJS*, 225, 5  
Chatterjee S., et al., 2017, *Nature*, 541, 58  
Connor L., Pen U.-L., Oppermann N., 2016, *MNRAS*, 458, L89  
Cordes J. M., Lazio T. J. W., 2002, ArXiv Astrophysics e-prints arXiv:astro-ph/0207156,  
Deneva J. S., et al., 2009, *ApJ*, 703, 2259  
Farah W., et al., 2018, *MNRAS*, 478, 1209  
Gajjar V., et al., 2018, *ApJ*, 863, 2  
Hay S. G., O’Sullivan J. D., 2008, *Radio Science*, 43, RS6S04  
Hotan A. W., et al., 2014, *PASA*, 31, e041  
Ioka K., 2003, *ApJL*, 598, L79  
James C. W., 2019, preprint, ([arXiv:1902.04932](https://arxiv.org/abs/1902.04932))  
James C. W., et al., 2018, preprint, ([arXiv:1810.04356](https://arxiv.org/abs/1810.04356))  
Keane E. F., et al., 2018, *MNRAS*, 473, 116  
Keith M. J., et al., 2010, *MNRAS*, 409, 619  
Law C. J., et al., 2017, *ApJ*, 850, 76  
Macquart J.-P., et al., 2010, *PASA*, 27, 272  
Mahony E. K., et al., 2018, *ApJ*, 867, L10  
Manchester R. N., et al., 2001, *MNRAS*, 328, 17  
McQuinn M., 2014, *ApJL*, 780, L33  
Michilli D., et al., 2018, *Nature*, 553, 182  
Oppermann N., Yu H.-R., Pen U.-L., 2018, *MNRAS*, 475, 5109  
Patel C., et al., 2018, *ApJ*, 869, 181  
Petroff E., et al., 2016, *PASA*, 33, e045  
Planck Collaboration et al., 2016, *A&A*, 594, A13  
Price D. C., et al., 2018, *Research Notes of the American Astronomical Society*, 2, 30  
Ravi V., et al., 2016, *Science*, 354, 1249  
Scholz P., et al., 2016, *ApJ*, 833, 177  
Shannon R. M., et al., 2018, *Nature*, 562, 386  
Spitler L. G., et al., 2014, *ApJ*, 790, 101  
Spitler L. G., et al., 2016, *Nature*, 531, 202  
Spitler L. G., et al., 2018, *ApJ*, 863, 150  
Stovall K., et al., 2014, *ApJ*, 791, 67  
Tendulkar S. P., et al., 2017, *ApJ*, 834, L7  
Walker C. R. H., Ma Y.-Z., Breton R. P., 2018, preprint, ([arXiv:1804.01548](https://arxiv.org/abs/1804.01548))  
Wright E. L., et al., 2010, *AJ*, 140, 1868  
Xu J., Han J. L., 2015, *Research in Astronomy and Astrophysics*, 15, 1629  
Yao J. M., Manchester R. N., Wang N., 2017, *ApJ*, 835, 29  
Zackay B., Ofek E. O., 2017, *ApJ*, 835, 11  
Zhang Y. G., Gajjar V., Foster G., Siemion A., Cordes J., Law C., Wang Y., 2018, *ApJ*, 866, 149  
Zhou B., Li X., Wang T., Fan Y.-Z., Wei D.-M., 2014, *Phys. Rev. D*, 89, 107303

This paper has been typeset from a  $\text{\TeX}/\text{\LaTeX}$  file prepared by the author.